Varying QD polymer coating effects on inflammatory and cytoskeletal changes in mammalian cells

Bella B. Manshian[1*], Abuelmagd M. Abdelmonem[2], Karsten Kanker[2], Beatriz Pelaz[2], Markus Klapper[3], Catarina NardiTironi[3], Wolfgang J. Parak[2,4], Uwe Himmelreich[1], Stefaan J. Soenen[1]

[1]Biomedical NMR Unit/MoSAIC, KULeuven Campus Gasthuisberg, Radiology Department, Herestraat 49, Leuven B3000, Belgium.

[2]Department of Physics, Philipps University of Marburg, Renthof 7, D-35037 Marburg, Germany.

[3]Max Planck Institute for Polymer Chemistry, Mainz, Germany

[4]CIC biomaGUNE, San Sebastián, Spain.

Corresponding author: bella.manshian@kuleuven.be

Biomedical NMR Unit/MoSAIC, KULeuven Campus Gasthuisberg, Radiology Department, Herestraat 49, Leuven B3000, Belgium.

Tel: +32 16 330034

Fax: +32 16 345991

Keywords: Quantum dot, polymer coating, cellular uptake, toxicity

Abstract

While substantial progress has been achieved in the design of biocompatible polymers for coating QDs, yet, for this field to advance further and to meet the future research challenges and developments in biomaterial and biosensor technologies it is important to improve our understanding of the cellular interactions of QDs when coated with different polymers. Therefore, the present study aimed to investigate the interaction of two quantum dots (QD) of the same core material CdSe/ZnS coated with two different amphiphilic polymers; PMA and PTMAEMA-stat-PLMA carrying negative and positive charge respectively, with two well-established mammalian cells; the human bronchial epithelial (BEAS-2B) and foreskin fibroblasts (HFF-1) exploring the internalization, effects on the cellular homeostasis, and consequent inflammatory and cytoskeletal alterations. Advanced fluorescence imaging techniques including; image-based flow cytometry, high-content imaging, and confocal microscopy were used in a multiparametric methodology to evaluate cell viability, induction of oxidative stress, mitochondrial health, cell cytoskeletal functionality, and changes in cellular morphology. Gene expression arrays were carried out on 168 key genes involved in the cytoskeletal architecture and inflammatory pathway accompanied with the analysis of focal adhesions as key markers for actin-mediated signaling. Our results show a distinct difference between the negatively charged PMA and positively charged PTMAEMA-stat-PLMA QDs. Both QDs triggered alterations to important but different genes, most remarkably the significant up-regulation of tumor suppression and necrosis genes and the down regulation of angiogenesis and metastasis genes in cells exposed to sub-cytotoxic concentrations of QDs.

The field of nanotechnology is rapidly advancing and, the use of nanomaterials (NMs) for biomedical purposes is gaining great interest [1]. A wide variety of nanosized materials are

currently being explored for their biotechnological use, offering a broad range of potentially useful physical and chemical properties that are unique to these NMs, and could revolutionize several fields of biomedicine [1-3]. Quantum dots (QDs) are an example of NMs that offer promising properties, though further effort is required to make them safe for biomedical use [4]. Owing to their high brightness, broad excitation and size-tunable emission spectra, multiple sized QDs can all be excited with a single excitation source, resulting in efficient multiplexing and simultaneous detection of a multitude of markers in a single specimen, such as clinical tissue sections [5, 6]. These unique fluorescent properties have made QDs valuable tools in biomedical research, where they have frequently been employed in staining fixed cells and tissues, showing in some cases better detection than possible with organic fluorophores [5, 7-10]. The increasing use of NMs and the strong focus to employ them as biological and medical research tools have emphasized the importance of a better understanding of the existence of possible health effects that these NMs may exert [11] and the mechanisms by which they interact with the intracellular environment. The toxic effects of QDs have already been explored in numerous studies, in vitro [16-18] as well as in vivo [19]. The presence of free cadmium ions due to low pH in the endosomal and lysosomal environment, and the induction of oxidative stress have been correlated with their toxicity [18-21]. However, any straightforward analysis of obtained results is made complex by, amongst others, the wide variety in the different materials used for QD synthesis, the presence or absence of a passivating shell layer on top of the QD core, and differences in the nature of the coating used for colloidal stability in an aqueous environment [12]. Although important progress has been made in the field of nanotoxicology, key questions such as the role of the intricate physicochemical properties of NPs such as size, shape or charge on cellular interactions are only partly understood [13]. The ambiguity in the obtained results can partially be explained in terms of difficulties in preparing different NPs that vary in only a single physicochemical property, as these are often interrelated

[13]. Furthermore, many studies focus on only a few selected parameters [14, 15].However, as NMs are known to interact with cells through various possible mechanisms, a proper understanding of the contribution of a single physicochemical parameter on how the cell will interact with this NM requires an in-depth study, where a full overview must be obtained in terms of NP properties and the likelihood of NP degradation in biological environments, cellular uptake, cytotoxicity, genotoxicity, morphological and gene expression changes.

Clearly, one major topic of interest is the effect of surface coating on the cellular interaction of QDs. Some studies have already been undertaken, where often commercially obtained or in-house prepared QDs were used, in which the surface charge is introduced *via* carboxyl or amine moieties on the surface ligands [15, 20]. However, the protonation state and thus the resulting net charge of NPs is dependent on the surrounding pH, which may drop from above 7 down to around 2 upon passage from the cell culture media into endosomal and lysosomal environments during cellular internalization *via* endocytosis. These environmental factors can influence the surface charge which subsequently can drastically affect the colloidal stability of the NMs [22]. Recently, a strategy was developed based on encapsulating NPs by amphiphilic diblock-copolymers [23]. These diblock-copolymers contain blocks of monomers with long alkyl side chains and blocks of monomers that through charged groups provide solubility in aqueous solution. Phosphonate and trimethylammonium groups, for example provide, a permanent negative and positive charge under physiologically relevant conditions, respectively [24]. For both, negatively and positively charged NPs, the charged groups are situated on the same polymer backbone, and colloidal stability of both NPs under different serum levels is similar [24]. The polymers used here were the poly(isobutylene–alt–maleic anhydride)–graft–dodecyl (PMA) and poly(N,N,N-trimethylamonium-2-ethyl methacrylate iodide)x-stat-poly(lauryl methacrylate)y (PTMAEMA-stat-PLMA) for the negatively and positively charged QDs

respectively. These polymers have previously demonstrated to be good coatings for NP stability and comparatively limited toxicity in mammalian cells [Guillaume O, MacromolBiosci. 2012].

The present work aims to characterize the interactions of PMA coated negatively charged and PTMAEMA-stat-PLMA coated positively charged QDs (from now on to be referred to as PMA and PLMA QDs), with the same core differing in first order only in their surface coating and charge, with two human exposure relevant, well established, mammalian cell lines; BEAS-2B (bronchial epithelial cells) and HFF-1 (skin fibroblasts). QD uptake and toxicity were examinedat a single cell and overall population level. Advanced fluorescence imaging techniques were used to evaluate cellular uptake and cytotoxicity of these QDs. A multiparametric methodology has been employed to evaluate NP toxicity and cell stress[25] taking into account intracellular QD localisation and the effect of the cellular environment on the QD fluorescence degradation. Cell viability, induction of reactive oxygen species, mitochondrial oxidative stress, cellular cytoskeletal health, and changes in cell morphology were performed. After these experiments, in-depth functional studies were performed to better understand the mechanisms underlying the observed effects. Pathway based gene expression arrays were performedon genes involved in the cytoskeletal structureand associated signaling and inflammation. Actin mediated signaling of focal adhesionswere determined. Finally, the respective impact of the difference in surface charge between the colloidal QDs was analyzed for each investigated parameter.

Materials and Methods

Cell culture

Human bronchial epithelial BEAS-2B cells (ATCC, UK, CRL-9609) and human foreskin fibroblasts HFF-1 cells (ATCC, UK, SCRC-1041) were maintained in 75 cm^2 flasks. BEAS-2B and HFF-1 cells were grown in Dulbecco's Modified Eagle's Medium (DMEM) in the presence of 10% and 15% fetal bovine serum (FBS, Gibco, Life Technologies, Belgium) consecutively. All cells were incubated in an atmosphere of 37 °C and 5% CO_2 and sub-cultured every other day for BEAS-2B cells and every three days for HFF-1 cells.

Quantum dots

Monodisperse red fluorescent CdSe/ZnS core/shell QDs with spherical shape were synthesized as reported elsewhere [26]. The negatively charged amphiphilic polymer consisted of poly(isobutylene–alt–maleic anhydride)–graft–dodecyl (PMA) while the positively charged amphiphilic polymer comprised of poly(N,N,N-trimethylamonium-2-ethyl methacrylate iodide)x-stat-poly(lauryl methacrylate)y(PTMAEMA-stat-PLMA, x/y = 53/47(see the Supporting Information for details).

Cell viability assays

Cell viability was examined and quantitative data were generated using the colorimetric 3-(4,5-dimethylthiazol-2-yl)-2,5-diphenyl tetrazolium bromide (MTT) assay according to Mosmann[31] and the InCell high throughput analysis method as previously described [Manshian Biomaterials 2014] (for details see supplementary materials).

Cellular uptake analysis

The ImageStream high throughput semi-quantitative image based flow cytometry was used to determine the uptake of the QDs into BEAS-2B or HFF-1 cells. Cells were seeded at $1.5x10^5$ cells/mL in 10 mL total culture medium and allowed to settle overnight in a humidified incubator at 37 ^oC. Both, BEAS-2B and HFF-1 cells were used for experimentation when approximately 70% confluent. Cells were then treated with 0, 5, 10, 15, 20, and 30 nM concentrations of QDs for 24 h. Following the exposure period, treated cells were washed twice with PBS and fixed with FACS fix (BD Biosciences, Belgium) for 30 min. Cell pellets were resuspended in 100 µL PBS and fluorescence intensity was excited with a 488 nm laser lamp and collected at 633 nm. All experiments were conducted in triplicates accompanied with a parallel sample of negative, water control. Data were analysed using the IDEAS v5 software (Amnis Corporation) and results were represented as the mean $\pm$ standard error to the mean of fluorescence intensity levels relative to the untreated control.

Next, inductively coupled plasma mass spectroscopy (ICP-MS) was conducted in order to determine the number of QDs per cell. For this end, cells were labeled with QDs at the above specifiedconcentrations for 24 hr. Cells were then washed thoroughly and counted using aBurkercell counter following which they were fixed in 4% paraformaldehyde. Number of cadmium and selenium atoms per cell were determined using ICP-MS (see supplementary information for more details).

Mechanistic studies

Analysis of cellular reactive oxygen species and mitochondrial membrane permeability were performed as previously described [ManshianBiomat, ManshianToxSci]. BEAS-2B and HFF-1 cells seeded in dark 96-well plates were treated with the QDs at the above listed concentrations and incubated for 24 h. Following the exposure period cells were washed and

stained with CellROX Green (Molecular Probes Europe, BV, Belgium). For the InCell based analysis cells were seeded in 24-well plates and stained with CellROX Green and MitoTracker Red CMXRos (Molecular Probes Europe, BV, Belgium). Fluorescence intensity was determined using an Omega plate reader (BMG Labtech, UK) while InCell image acquisition took place on an InCell analyzer 2000 (GE Healthcare, Belgium) (for more details see supplementary information).

Changes to cytoskeletal proteins

To analyze the effects of QDs on BEAS-2B and HFF-1 cell focal adhesions, confocal microscopy was conducted as previously described[25]. For this end, cells were incubated with primary anti-vinculin mouse monoclonal (no. ab18058, 1:200; Abcam, Cambridge, UK), secondary Alexa Fluor 488-conjugated goat anti-mouse (Molecular Probes, Leiden, Netherlands) and Alexa Fluor 546-conjugated phalloidin (Molecular Probes, Leiden, Netherlands) antibodies. High content image analysis using InCellanalyser 2000 was also conducted to examine morphological changes using primary anti-tubulin (Abcam, Cambridge, UK), secondary Alexa Fluor 488-conjugated goat anti-mouse (Molecular Probes, Life Technologies Europe, BV, Belgium), and AF568-coupled phalloidin (Molecular Probes, Life Technologies Europe, BV, Belgium) antibodies (For more details see supplementary material).

RT-PCR arrays

Two RT-PCR gene expression pathway arrays were used. These were the human cytoskeletal regulator array (PAHZ-088Z, QiagenBenelux BV, Netherlands) and the inflammatory cytokines and receptors array (PAHS-011Z, Qiagen Benelux BV, Netherlands). Both arrays

were prepared and processed similarly (see supplementary material).PCR array data was analysed using the $\Delta\Delta C_t$ method via the SABiosciencesweb portal (www.SABiosciences.com/pcrarraydataanalysis.php).

Statistical analysis

All data are expressed as the mean ± standard error of the mean (SEM). All experiments, except the PCR arrays, were analysed using the T-test statistical method. Significance in the PCR arrays was determined based on 2-fold change from the control $\Delta\Delta C_t$ value.

Results

Characterization of QD NPs

The QDs used in this study consisted of spherical CdSe/ZnS core-shell structures initially capped with a hydrophobic surfactant. TEM imaging determined thediameterof the inorganic core-shell to be; d_c=.4.6 ± 0.9 nm for the PMA and d_c=4.5± 0.8 nm for the PLMA QDs. These QDs were overcoated with PMA and PTMAEMA-stat-PLMAamphiphilic polymer molecules to render these QDs (see supplementary information). The final hydrodynamic diameter of the polymer coated QDs, as determined by dynamic light scattering (DLS), in PBS was dh = 11.9 ± 5.6 nm and dh = 11.0 ± 4.2 nm and a zeta potential of ζ = - 29.0±5.6 mV and ζ = + 30.8±6.8 mV for the PMA and PLMA QDs consecutively.

Cellular uptake

As shown in **Table 1**, BEAS-2B and HFF-1 cells treated with PLMA or PMA QDs exhibited dose-dependent increase of their mean fluorescence intensity over the control samples. Uptake was significantly different than the control from both NPs in both cell types even at the lowest concentration of 5 nM, where uptake was increased by approximately 2-fold (BEAS-2B), 3-fold (HFF-1), and 4-fold (BEAS-2B), 6-fold (HFF-1) for the PLMA and PMA QDs,respectively. Interestingly, increasing PMA QD concentrations resulted in higher total uptake levels at 30 nM(6-fold increase in BEAS-2B and 19-fold in HFF-1 cells), but the extent of QD uptake was much lower when compared to the P QDs at the same concentration (11-fold increase in BEAS-2B and 63-fold in HFF-1 cells).

The above results showed clear differences in fluorescence (cellulardose) between the QDs, however, the cellular dose did not appear to bedirectly proportional to the nominal media concentration,specifically, at the top three exposure concentrations. Thus, in order to better understand the role of the cellular internalisation of QDs on the observed effects in this study, ICP-MS analysis was used to determine number of QD NPs per cell. These data were similar to the ImageStream results where higher numbers of PLMA QDs were internalised compared to PMA QDs in both BEAS-2B (e.g. 37768.6 vs 736.0 at 30nM) and HFF-1 (e.g. 34192.2 vs 813.4 at 30 nM) cells. However, in general, the number of QDs internalised by both cell types was not directly proportional to the exposure concentration, especially in the case of the PMA QDs (Table S1). Therefore, toxicity data have been presented in terms of intracellular QD numbers as well as exposure concentration. Corresponding graphs with concentration values can be found in the supplementary materials section.

Cytotoxic effects of QD exposure

MTT assay results showed that BEAS-2B and HFF-1 cells treated with QDs up to 50nM tolerated exposure to the PMA and PLMA QDs up to 20 nM concentration (**Figure 1A, 1B**). Cell survival was significantly compromised at doses above 40 nM from both QDs in both cell types (Figure S2).No significant difference was noted from exposure of the cells to either QD.

Cell viability was then also quantified through staining QD-exposed cells with calcein AM and far red dead cell stain followed by high-content (HC) quantitative imaging (**Figure 1C, 1D**). For both cell types, no toxic effects were observed for the PMA QDs up to 30 nM except for significant toxicity noted in BEAS-2B cells treated with the PMA QDs at 30nM concentration.

Oxidative damage

A clear, dose-dependent, increase in ROS was seen in both cell types from both NPs using the CellROX chemiluminescent assay system (**Figure 2A, 2B**). Here we see that ROS levels were slightly higher in HFF-1 cells exposed to PLMA QDs (approximately 2.8-fold higher than the control level at 20nM), while BEAS-2B cells exposed to the same QDs at the same concentration induced 2.2-foldmore ROS compared to the controls.

Next HC-analysis was performed on both cells following exposure to the QDs. Cells were stained for cellular and Mitochondrial ROS detection (**Figure 2C, 2D)**. Data revealed a significant, dose-dependent, increase in cellular ROS in both cells exposed to the PLMA QDs. The only significant increase in ROS levels noted from exposure to the PMAQDs were in BEAS-2B cells at 30 nM concentration. The mitochondrial stain revealed a clear QD-related increase in the level of mitochondrial-based ROS, especially for the PLMA QDs. The PMAQDs were more cell type dependent with significant levels of mitochondrial ROS detected in BEAS-2B cells but not in HFF-1 cells.

Effects of QD labeling on cellular morphology

Focal adhesions

As a general marker for focal adhesions, QD-exposed BEAS-2B and HFF-1 cells were stained for vinculin, after which the total cellular size of the focal adhesions was calculated after confocal analysis (**Figure 3A, 3B**). The data show that HFF-1 cells contain more focal adhesions than BEAS-2B cells. The overall size of the focal adhesions was only minimally affected by the PMA QDs at concentrations up to 20 nM. PLMA QDs significantly affected focal adhesion size from 10 nM and higher for BEAS-2B cells and at concentrations as low as 5 nM for HFF-1 cells.

Cytoskeletal changes

For this analysis both BEAS-2B and HFF-1 cells were exposed to PMA and PLMA QDs, after which the cells were stained for α-tubulin, F-actin and cytoplasm. Cells were permeabilized, blocked and stained with antibodies. The cells underwent multiple thorough washing steps, hereby removing dead cells that detach from the well ruling out their influence on the results obtained. Using HC-based imaging, the morphology of both cell types was found to be significantly affected (**Figure 3C, 3D**). For PMA QDs, a clear decrease in cell spreading is observed at 30 nM, where PLMA QDs displayed a clear concentration-dependent decrease in cell spreading starting from 15 nM.

Gene alterations

For this section cytoskeletal regulator gene arrays were performed in both BEAS-2B and HFF-1 cells exposed to either QD. Different genes were up or down regulated in each of the cell types. PMA QDs showed minimal effects on gene expression, which is in line with the data obtained above. Contrarily, PLMA QDs resulted in far greater levels of gene alterations (**Figure 4**). The data reveal that IQGAP2 gene was significantly upregulated in both cell types exposed to 20nM of PLMA QDsyet cells exposed to the PMA QDs showed either slight reduction or no notable alteration in the expression of the IQGAP2 gene.

Other genes that were significantly over expressed in BEAS-2B cells following exposure to the PLMAQDs were: ARAP1, ARFIP2, ARHGAP6, ARHGDIB, ARHGEF11, MYLK2, and WAS genes. These genes showed slightly increased expression in HFF-1 cells (see supplementary materials **Table S1**) from both QDs yet they were significantly overexpressed in BEAS-2B cells exposed to both QDs.

In addition to the above mentioned genes, a few other genes being; ACTR3, ARPC2, and RDX presented with differential expression in HFF-1 cellsfollowing incubation with either QD. Contrary to HFF-1 cells these genes were not altered in BEAS-2B cells.

Inflammatory effects of QD labeling

To gain more insight into this phenomenon, RT-PCR array analysis for the inflammatory cytokine regulator pathway was performed. **Figure 6** displays a significant number of genes that were upregulated in the HFF-1 cells treated with 20 nM concentration of either the PMAor PLMA QDs. One major difference between the two NPs is that the PMA QDs induced highly significant overexpression of the CCR2 gene with 38- and 89- fold increase over the control treatments compared to only 5-fold increase in the same cells exposed to the PLMA QDs.

CXCL9 has increased by 16-fold in 20 nMPMA QD and 3-fold in PLMA QD treatments. IFNα2b is yet another interferon that was found overexpressed with both NPs with higher expression seen with PLMA QDs (12-fold) than with PMA QDs (5-fold). IL17F was highly expressed in cells treated with either type of QDs at 13-fold (PLMA QD) and 15-fold (PMA QD) increase compared with controls. Most interestingly, cells exposed to both QDs showed a substantial down regulation of genes in the TNF family, CXCL1, and VEGFA genes.

Discussion

Coating QDs with polymers, such as; PMA and PTMAEMA-stat-PLMA, used in this study, has been shown to result in excellent NP colloidal stability [NikodemTomczakand Parak, Nanoscale 2013]. However, when in the intracellular environment, NPs are influenced by low pH conditions that can result in changes to their surfacechemistry leading to undesired toxic effects. Thus here, the two abovementioned polymers were used to coat the same CdSe/ZnS core QDs and to study the effect of changing polymer coatings on the observed biological outcomes.

Thus, in this study, we have used regular chemiluminescent assays along with a high-content (HC) imaging technique previously established [Bella Biomaterials 2014] to investigate the effects of the interaction of two different polymer based QDs on cellular homeostasis. The HC based imaging setup was utilized because it allows for rapid evaluation of QD toxicity and provides large datasets that enable more statistically robust analysis. Furthermore, the analysis itself provides an overview of the entire population, where the distribution of a certain parameter over the entire population can be obtained that is then represented by the standard deviation. This is in contrast to most biochemical assays where a single average value is obtained and standard deviations represent differences between replicates.

Initially, we explored the effects of changing pH levels on the degradation of these NPs. Non-significant, time-dependent (after 5 days) loss of fluorescence intensity was noted from both QDs which could be linked to partial breakdown of the QDs due to photo-oxidation [36]. The loss of fluorescence at the later time points may suggest particle degradation which could possibly lead to the release of Cd^{2+} ions, which may contribute to their overall toxicity [20]. However, as both NPs display similar effects, the surface coating of the QDs does not seem to affect their chemical stability against pH-induced degradation, in particular as in the case of the here used polymer-coated QDs both types of QDs have exactly the same ligands, hexydecylamine (HDA) and trioctylphosphineoxide (TOPO) directly linked to the QD surface beneath the terminating amphiphilic polymer coating of either positive or negative charge. Considering that these QDs were covalently bound with amine and carboxylic acid (which provided their charge) which could result in a different zeta potential in low pH levels we therefore suggest that any toxic effects observed should not be predominantly related to intrinsic differences in Cd^{2+} release kinetics, but will be linked to other factors that may be directly influenced by the NP surface coating (e.g. cellular uptake, membrane damage). We continue referring to the QDs based on their charge for ease of presentation.

To confirm internalization of both QDs by the BEAS-2B and HFF-1 cells, ImageStreamhigh throughput image-based flow cytometry was used. This system allowed the acquisition of semi-quantitative and image-confirmed information on the uptake of the QDs. We were able to acquire integrated fluorescence signals in addition to high quality fluorescence images of a large population of cells (5000 cells per replicate) which provides it with statistical robustness. The IDEAS v 5.0 analysis software which allows for the selection of single cells that are in focus, to confirm the accurate imaging acquisition of the interior of the cells[37], was used for the processing of the collected data. In general, PLMA QDs were more freely taken up by both cells and some difference was noted between the cell types whereas HFF-1 cells allowed for

the internalization of more QDs compared to the BEAS-2B cells which could be related to the difference in the endocytic capacity of these cells [Paul Rees, Nature Methods, 2014].Some of the difference in cellular uptake levels could also be related to differences in the surface charge of the QDs. As previously reported, higher uptake levels were detected in positive QDs with the same surface coating compared to negative QDs, even when in high serum-containing media, which could obscure its positive surface potential [24].

The potential cytotoxic effects of the QDs were tested using two methods. The first method, the MTT assay, is a colorimetric assay where viable cells produce mitochondrial dehydrogenases which convert the yellow soluble MTT solution into blue-violet insoluble formazan crystals that can be quantified by measuring the optical density of the cells. MTT assay results showed tolerance of both QDs by both cell types up to 20 nM concentration. InCell HC analysis results also showed that both cells were able to tolerate exposure to either QDs up to 20 nM concentration. In the absence of significant cytotoxicity we investigated the presence of free radicals and other reactive oxygen species (ROS) which have been described as a major effect of NMs on cultured cells [40]. ROS are known to be generated in cells exposed to QDs [20] and this phenomenon has been related to NP uptake levels, which is in line with our findings as we noted higher induction of ROS in cells exposed to the PLMA QDs than the PMA QDs. These results were further validated with high content image analysis where approximately 15000 cells were analyzed per condition. These analyses exhibited similar results to the ones seen with the CellROX system. A dose-dependent significant increase in cellular ROS were present from exposure to PLMA QDs yet PMA QDs induced ROS generation only at 30nM in BEAS-2B cells. This could be correlated to the cytotoxic damage noted in BEAS-B cells from exposure to the same concentration of the PMA QDs. Next, mitochondrial ROS were examined for secondary toxicity induced by the QDs. The results obtained showed a clear increase in mitochondrial ROS levels from both QDs. However, the PLMA QDs resulted in more elevated

mitochondrial ROS levels in both cell types more so in HFF-1 cells which could be explained by the substantially higher level of these NPs in these cells. The values obtained from this analysis were generally much higher than the values for cellular ROS as obtained by the CellROX reagent, indicating a clear effect of the QDs on mitochondrial metabolism. These values might also in part explain the high results obtained by the MTT assay, which measures mitochondrial metabolism. The higher ROS levels might induce cellular stress and increase the activity of mitochondrial enzymes, therefore obscuring any toxic effects. The PMA QDs used here were previously used in PC12, HUVEC, and C17.2 cells [18] where similar to our BEAS-2B results, a decrease in cell viability was observed at 30nM dose which appeared to be correlated to the increase in the generation of ROS and mitochondrial ROS. Soenen *et al* also reports a lack of significant effect on cellular morphology following exposure of the cells tothese QDs [18] which is comparable to our results.

As the HC imaging results indicate cytoskeletal aberrations and mitochondrial ROS to be key pathways in the toxic effects of the QDs, additional in-depth studies were performed to reveal possible functional consequences of these effects and to better understand the mechanisms underlying these observations. Several studies have found that NP-induced alterations in cytoskeletal architecture can result in functional effects, such as reducing cellular migration [42] or proliferation and differentiation of mesenchymal stem cells [43]. Therefore, the functional effect of these alterations was assessed, by analyzing the size of the focal adhesions, which are key mediators in actin-mediated signaling [44], and have been described to be affected upon NP-mediated disturbance of the actin cytoskeleton [45]. The higher sensitivity of the HFF-1 cells might be explained by the overall higher level of focal adhesions in these cells. These data clearly indicate substantial effects of the PLMA QDs on focal adhesions at relatively low QD concentrations, indicating potential functional defects at sub-cytotoxic concentrations.Next, changes to cytoskeletal proteins were examined by staining for tubulin, F-

actin. The data indicated a clear link between the number of cell-associated QDs and the effects of the QDs on cell morphology since PLMA QDs, which were more readily taken up by both cells, caused significant changes to the cellular morphology. These effects were less pronounced in cells exposed to the PMA QDs which was, also, less internalized by both cells. These findings are in line with various previous reports, where inorganic NPs, including QDs, have been found to affect cell cytoskeletal structure [20, 25].

Beside cytoskeletal aberrations, the induction of mitochondrial ROS has been found to be a major pathway in the observed cytotoxicity of the QDs. As mitochondrial ROS has been linked to the induction of pro-inflammatory cytokines, the effect of the QDs on the production of IL-8 was explored (supplementary materials **Figure SI-XIII**). We noted significant increase in the induction of these cytokines in cells exposed to the PLMA QDs which is in line with the results obtained in the next analysis, RT-PCR of inflammatory and cytoskeletal regulator pathways. For this analysis three concentrations of QDs were used; 0 for control, 5 nM representing the lowest concentration and 20 nM representing a high concentration at which significant cellular changes have been observed in other tests in both cell types and where differences between types of QDs exist yet no significant cytotoxicity was detected.

IQGAP2, an IQ Motif Containing GTPase activating protein which regulates cell morphology and motility [46-48] was found elevated in these treatments. This gene has been implicated in cadherin-mediated cell adhesion [49], suppression of prostate cancer [46] and depleted values were reported in hepatocellular carcinoma [47]. ARAP1, ARFIP2, ARHGAP6, ARHGDIB, ARHGEF11, MYLK2, and WAS genes. All of these genes are involved in the trafficking of molecules into the cell [52, 53], signaling from receptors on the cell surface to the actin cytoskeleton which influences the cell's ability to grow and proliferate [52, 54-57]. Other cytoskeletal gene alterations noted mainly in HFF-1 cells exposed to either QDs were Actin-Related Protein 3 Homolog (ACTR3), which encodes a protein known to be a major constituent

of the ARP2/3 complex, ARCP2 being a subunit of this complex, located at the cell surface playing an essential role in maintaining cell shape and motility. Radixin (RDX), which was reduced in HFF-1 cells, is a cytoskeletal protein that is thought to be important in linking actin to the plasma membrane was under-expressed in these cells. Though slight increase is noted in ACTR3 gene expression in HFF-1 cells however this was not accompanied by alterations in the ARCP2 nor RDX genes suggesting a difference in the mechanisms by which different cells process NPs with different surface properties. These genes were not effected in treatments in the BEAS-2B cells. These genes were found to be upregulated in all treatments but significant levels were only achieved by the PLMA QDs. This could be due to the PTMAEMA-stat-PLMA polymer coating of these QDs which enhances their uptake and thus their trafficking by genes specific for this purpose. Uptake data suggest that the extent of these effects is correlated to the level of intracellular QDs, being most evident for the positively charged PLMA QDs. Some differences between the two cell types also exist, both in the extent of the observed effects as well as in the nature of the genes affected. These differences between the BEAS-2B (significant changes with PLMA QDs) and HFF-1 cells (no or slight changes) could be due to the general expression of the above listed genes in the different human organs where less expression in general has been reported in skin cells than in lung cells [http://biogps.org/#goto=genereport&id=116985]. As a whole these findings suggest that these QDs have no undesired effects on cellular proliferation and instead they appear to be involved in the expression of important tumor suppression genes. Furthermore, it places an emphasis on the importance of studying multiple cell types in regards to their interaction with NPs, as data for one cell type cannot easily be transposed onto other cell types [58].

In the inflammatory cytokine expression array Chemokine (C-C motif) receptor 2 (CCR2) gene was upregulated following exposure to both QDs however the effects of the PMA QDs were substantially higher. This gene encodes a receptor which mediates monocyte chemotaxis [59].

CCR2 also havepro-inflammatory and anti-inflammatory roles in addition to playing an important part in mediating inflammatory responses against tumors [60, 62, 63]. Therefore, it is possible to assume that CCR2 over expression here is an indication of a cellular defense against possible inflammatory effects initiated by these QDs which has been previously suggested to be involved in recruiting macrophages which promote angiogenesis and thus tissue repair [64]. Similarly, Interferon-γ-inducible protein-9 (CXCL9) was found to be highly elevated in HFF-1 cells exposed to either QDs and decreased in HFf-1 cells indicating a cell specific effect in the expression of these genes. Two other key inflammatory genes that were found to be altered were; IFNα2b protein has been shown to be involved in recruiting natural killer (NK) cells and tumor-suppressive T-lymphocytes that hinder tumor growth and metastasis [68]. This gene is reported to be an effective immune stimulator [69] while IL17F, a cytokine that is usually expressed by activated T-cells, and associated with inflammation [70]. Both genes were found to be up-regulated from exposure to both QDs mainly in the HFF-1 cells. However, the most noteworthy changesnoted were the highly significant down regulation of major metastasis related genes such as the; TNF family, CXCL1, and VEGFA genes in cells exposed to the PMA QDS in BEAS-2B. Overall, some difference was noted in the inflammatory cytokine expression pattern between the two cells which could simply be related to their differential expression of these genes [Diana Lindner Biochemistry Research International 2012]. Most prominently, both QDs appear to affect key changes in the cells, which if examined further could become useful tools for therapeutic considerations.

Conclusions

The data obtained in the present study display clear contribution of the surface coating on theresultingbiologic effects. Overall, both QDs were not cytotoxic up to a concentration of

20nM. Cells exposed to the PTMAEMA-stat-PLMA coated positive QDs sustained more obvious changes to their natural homeostasis. PMA coated QDs were in general better tolerated by both cells. This difference could be due to the higher level of interaction of the PTMAEMA-stat-PLMA QDs with the cellular components and higher uptake levels. Overall, the extent of the toxic effects observed were similar for both cell types, despite large differences in their cellular QD uptake levels with some additional sensitivity noted in BEAS-2B cells. This clearly indicates differences in the intrinsic sensitivity of the cells to NPs. Exposure to these QDs mainly caused cytoskeletal aberrations and induction of mitochondrial ROS, which was primarily associated with PLMA charged QDs. However, even at lower intracellular NP levels, alterations in cell cytoskeleton resulted in many more genes being affected in the BEAS-2B cells than in the HFF-1 cells, confirming the higher sensitivity of the former cell type. Where cytoskeletal aberrations were clearly linked to the difference in the coating and most notable for the PLMA charged QDs, this was not the case for the inflammatory responses, where different patterns and different levels of alterations were observed between both types of QDs, and were most pronounced for the PMAcoated NPs.

Therefore, it was clear that generally PMA coating was more tolerated by cells. However both QDs demonstrated interesting influences on the gene regulation of the cells by inducing the up-regulation of tumor suppressor and necrosis genes and down regulation of tumor metastasis and angiogenesis genes which advocates for more detailed studies to further explore the exact role of these polymers in impeding tumorigenesis.

5. Acknowledgements

This work was supported by Flemish agency for Innovation by Science and Technology (IWT SBO MIRIAD/130065) and the KU Leuven program financing IMIR (PF 2010/017.SJS was

funded by the FWO-Vlaanderen. Beatriz Pelaz acknowledges a PostDoctoral fellowship from the Alexander von Humboldt Foundation. Parts of this project were funded by DFG GRK 1782 (grant to WJP).The authors are grateful to Dr. Christian Geidel for polymer synthesis in the exploratory stage of this project.

References

[1] Singh SK, Kulkarni PP, Dash D. Biomedical Applications of Nanomaterials: An Overview. In: Bagchi D, Bagchi M, Moriyama H, Shahidi F, editors. Bio-Nanotechnology: A Revolution in Food, Biomedical and Health Sciences. Oxford, U.K.: Blackwell Publishing, Ltd.; 2013.

[2] Ballou B, Lagerholm BC, Ernst LA, Bruchez MP, Waggoner AS. Noninvasive imaging of quantum dots in mice. Bioconjug Chem 2004;15:79-86.

[3] Liu J, et al. Assessing clinical prospects of silicon quantum dots: studies in mice and monkeys. ACS Nano 2013;7:7303-10.

[4] Winnik FM, Maysinger D. Quantum dot cytotoxicity and ways to reduce it. Acc Chem Res 2013;46:672-80.

[5] Wen X, et al. In vivo monitoring of neural stem cells after transplantation in acute cerebral infarction with dual-modal MR imaging and optical imaging. Biomaterials 2014;35:4627-35.

[6] Liu J, et al. Molecular mapping of tumor heterogeneity on clinical tissue specimens with multiplexed quantum dots. ACS Nano 2010;4:2755-65.

[7] Hahn MA, Keng PC, Krauss TD. Flow cytometric analysis to detect pathogens in bacterial cell mixtures using semiconductor quantum dots. Anal Chem 2008;80:864-72.

[8] Akinfieva O, Nabiev I, Sukhanova A. New directions in quantum dot-based cytometry detection of cancer serum markers and tumor cells. Crit Rev Oncol Hematol 2013;86:1-14.

[9] Clarke S, Pinaud F, Beutel O, You C, Piehler J, Dahan M. Covalent monofunctionalization of peptide-coated quantum dots for single-molecule assays. Nano Lett 2010;10:2147-54.

[10] Wu X, et al. Immunofluorescent labeling of cancer marker Her2 and other cellular targets with semiconductor quantum dots. Nat Biotechnol 2003;21:41-6.

[11] Zrazhevskiy P, Sena M, Gao X. Designing multifunctional quantum dots for bioimaging, detection, and drug delivery. Chem Soc Rev 2010;39:4326-54.

[12] Rivera Gil P, Oberdorster G, Elder A, Puntes V, Parak WJ. Correlating physico-chemical with toxicological properties of nanoparticles: the present and the future. ACS Nano 2010;4:5527-31.

[13] Rivera-Gil P, et al. The challenge to relate the physicochemical properties of colloidal nanoparticles to their cytotoxicity. Acc Chem Res 2013;46:743-9.

[14] Tang Y, et al. The role of surface chemistry in determining in vivo biodistribution and toxicity of CdSe/ZnS core-shell quantum dots. Biomaterials 2013;34:8741-55.

[15] Roberts JR, et al. Lung toxicity and biodistribution of Cd/Se-ZnS quantum dots with different surface functional groups after pulmonary exposure in rats. Part Fibre Toxicol 2013;10:5.

[16] Manshian BB, et al. Single-walled carbon nanotubes: differential genotoxic potential associated with physico-chemical properties. Nanotoxicology 2013;7:144-56.

[17] Smith WE, et al. In vitro toxicity assessment of amphiphillic polymer-coated CdSe/ZnS quantum dots in two human liver cell models. ACS Nano 2012;6:9475-84.

[18] Soenen SJ, et al. The effect of nanoparticle degradation on poly(methacrylic acid)-coated quantum dot toxicity: the importance of particle functionality assessment in toxicology. Acta Biomater 2014;10:732-41.

[19] Derfus AM, Chan WCW, Bhatia SN. Intracellular delivery of quantum dots for live cell labeling and organelle tracking. Advanced Materials 2004;16:961-+.

[20] Soenen SJ, Demeester J, De Smedt SC, Braeckmans K. The cytotoxic effects of polymer-coated quantum dots and restrictions for live cell applications. Biomaterials 2012;33:4882-8.

[21] Chen N, et al. The cytotoxicity of cadmium-based quantum dots. Biomaterials 2012;33:1238-44.

[22] Pellegrino T, Kudera S, Liedl T, Munoz Javier A, Manna L, Parak WJ. On the development of colloidal nanoparticles towards multifunctional structures and their possible use for biological applications. Small 2005;1:48-63.

[23] Pellegrino T, et al. Hydrophobic nanocrystals coated with an amphiphilic polymer shell: A general route to water soluble nanocrystals. Nano Letters 2004;4:703-7.

[24] Huhn D, et al. Polymer-coated nanoparticles interacting with proteins and cells: focusing on the sign of the net charge. ACS Nano 2013;7:3253-63.

[25] Soenen SJ, Rivera-Gil P, Montenegro JM, Parak WJ, De Smedt SC, Braeckmans K. Cellular toxicity of inorganic nanoparticles: Common aspects and guidelines for improved nanotoxicity evaluation. Nano Today 2011;6:446-65.

[26] Reiss P, Bleuse J, Pron A. Highly luminescent CdSe/ZnSe core/shell nanocrystals of low size dispersion. Nano Letters 2002;2:781-4.

[27] Lin CA, et al. Design of an amphiphilic polymer for nanoparticle coating and functionalization. Small 2008;4:334-41.

[28] Geidel C, et al. A general synthetic approach for obtaining cationic and anionic inorganic nanoparticles via encapsulation in amphiphilic copolymers. Small 2011;7:2929-34.

[29] Rivera-Gil P, Yang F, Thomas H, Li L, Terfort A, Parak WJ. Development of an assay based on cell counting with quantum dot labels for comparing cell adhesion within cocultures. Nano Today 2011;6:20-7.

[30] Yu WW, Qu LH, Guo WZ, Peng XG. Experimental determination of the extinction coefficient of CdTe, CdSe, and CdS nanocrystals. Chemistry of Materials 2003;15:2854-60.

[31] Mosmann T. Rapid colorimetric assay for cellular growth and survival: application to proliferation and cytotoxicity assays. J Immunol Methods 1983;65:55-63.

[32] Kirchner C, et al. Cytotoxicity of colloidal CdSe and CdSe/ZnS nanoparticles. Nano Lett 2005;5:331-8.

[33] Shi XL, et al. Rhodamine-based fluorescent probe for direct bio-imaging of lysosomal pH changes. Talanta 2014;130:356-62.

[34] Tycko B, Maxfield FR. Rapid Acidification of Endocytic Vesicles Containing Alpha-2-Macroglobulin. Cell 1982;28:643-51.

[35] Susha AS, Javier AM, Parak WJ, Rogach AL. Luminescent CdTe nanocrystals as ion probes and pH sensors in aqueous solutions. Colloids and Surfaces a-Physicochemical and Engineering Aspects 2006;281:40-3.

[36] Aldana J, Wang YA, Peng X. Photochemical instability of CdSe nanocrystals coated by hydrophilic thiols. J Am Chem Soc 2001;123:8844-50.

[37] Vranic S, et al. Deciphering the mechanisms of cellular uptake of engineered nanoparticles by accurate evaluation of internalization using imaging flow cytometry. Part Fibre Toxicol 2013;10:2.

[38] Hsiao IL, Huang YJ. Improving the interferences of methyl thiazolyl tetrazolium and IL-8 assays in assessing the cytotoxicity of nanoparticles. J Nanosci Nanotechnol 2011;11:5228-33.

[39] Chang E, Thekkek N, Yu WW, Colvin VL, Drezek R. Evaluation of quantum dot cytotoxicity based on intracellular uptake. Small 2006;2:1412-7.

[40] Nel A, Xia T, Madler L, Li N. Toxic potential of materials at the nanolevel. Science 2006;311:622-7.

[41] Freese C, et al. Uptake and cytotoxicity of citrate-coated gold nanospheres: Comparative studies on human endothelial and epithelial cells. Part Fibre Toxicol 2012;9:23.

[42] Tay CY, et al. Nanoparticles strengthen intracellular tension and retard cellular migration. Nano Lett 2014;14:83-8.

[43] Hou YH, et al. Effects of titanium nanoparticles on adhesion, migration, proliferation, and differentiation of mesenchymal stem cells. International Journal of Nanomedicine 2013;8:3619-30.

[44] Lim ST. Nuclear FAK: a new mode of gene regulation from cellular adhesions. Mol Cells 2013;36:1-6.

[45] Soenen SJH, Nuytten N, De Meyer SF, De Smedt SC, De Cuyper M. High Intracellular Iron Oxide Nanoparticle Concentrations Affect Cellular Cytoskeleton and Focal Adhesion Kinase-Mediated Signaling. Small 2010;6:832-42.

[46] Yanyun X, et al. IQGAP2, A candidate tumour suppressor of prostate tumorigenesis. Biochimi Biophys Acta-Molecular Basis of Disease 2012; 1822: 875–884.

[47] White CD, et al. IQGAP1 and IQGAP2 are reciprocally altered in hepatocellular carcinoma. BMC Gastroenterol 2010;10:125.

[48] Yamashiro S, Abe H, Mabuchi I. IQGAP2 is required for the cadherin-mediated cell-to-cell adhesion in Xenopus laevis embryos. Dev Biol 2007;308:485-93.

[49] Yamashiro S, Abe H, Mabuchi I. IQGAP2 is required for the cadherin-mediated cell-to-cell adhesion in Xenopus laevis embryos. Developmental Biology 2007;308:485-93.

[52] Daniele T, Di Tullio G, Santoro M, Turacchio G, De Matteis MA. ARAP1 Regulates EGF Receptor Trafficking and Signalling. Traffic 2008;9:2221-35.

[53] Guo FJ, et al. Identification of Rho GTPase Activating Protein 6 Isoform 1 Variant as a New Molecular Marker in Human Colorectal Tumors. Pathology & Oncology Research 2010;16:319-26.

[54] Banerjee J, Wedegaertner PB. Identification of a novel sequence PDZ-RhoGEF that mediates interaction with the in actin cytoskeleton. Molecular Biology of the Cell 2004;15:1760-75.

[55] Sato R, et al. Impaired cell adhesion, apoptosis, and signaling in WASP gene-disrupted Nalm-6 pre-B cells and recovery of cell adhesion using a transducible form of WASp. International Journal of Hematology 2012;95:299-310.

[56] Soung YH, et al. Mutational analysis of the kinase domain of MYLK2 gene in common human cancers. Pathology Research and Practice 2006;202:137-40.

[57] Rosado LAR, Rodriguez-Canales J, Zhang BL. Association of D4-GDI expression with breast cancer progression. Cancer Biomarkers 2011;10:163-73.

[58] Stepkowski TM, Brzoska K, Kruszewski M. Silver nanoparticles induced changes in the expression of NF-kappaB related genes are cell type specific and related to the basal activity of NF-kappaB. Toxicol In Vitro 2014;28:473-8.

[59] Volpe S, Cameroni E, Moepps B, Thelen S, Apuzzo T, Thelen M. CCR2 Acts as Scavenger for CCL2 during Monocyte Chemotaxis. Plos One 2012;7.

[60] Chen MK, Yeh KT, Chiou HL, Lin CW, Chung TT, Yang SF. CCR2-64I gene polymorphism increase susceptibility to oral cancer. Oral Oncology 2011;47:577-82.

[62] Deshmane SL, Kremlev S, Amini S, Sawaya BE. Monocyte Chemoattractant Protein-1 (MCP-1): An Overview. Journal of Interferon and Cytokine Research 2009;29:313-26.

[63] Kim Y, Sung SSJ, Kuziel WA, Feldman S, Fu SM, Rose CE. Enhanced airway Th2 response after allergen challenge in mice deficient in CC chemokine receptor-2 (CCR2). Journal of Immunology 2001;166:5183-92.

[64] Yang YM, et al. Aberrant expression of chemokine receptor CCR4 in human gastric cancer contributes to tumor-induced immunosuppression. Cancer Science 2011;102:1264-71.

[68] Mukherjee KK, et al. IFN alpha 2b augments immune responses of cisplatin+5-fluorouracil treated tongue squamous cell carcinoma patients - a preliminary study. Indian Journal of Medical Research 2012;136:54-9.

[69] Krejsgaard T, et al. Elucidating the role of interleukin-17F in cutaneous T-cell lymphoma. Blood 2013;122:943-50.

[70] West NR, Murphy LC, Watson PH. Oncostatin M suppresses oestrogen receptor-alpha expression and is associated with poor outcome in human breast cancer. Endocrine-Related Cancer 2012;19:181-95.

Figure Legends

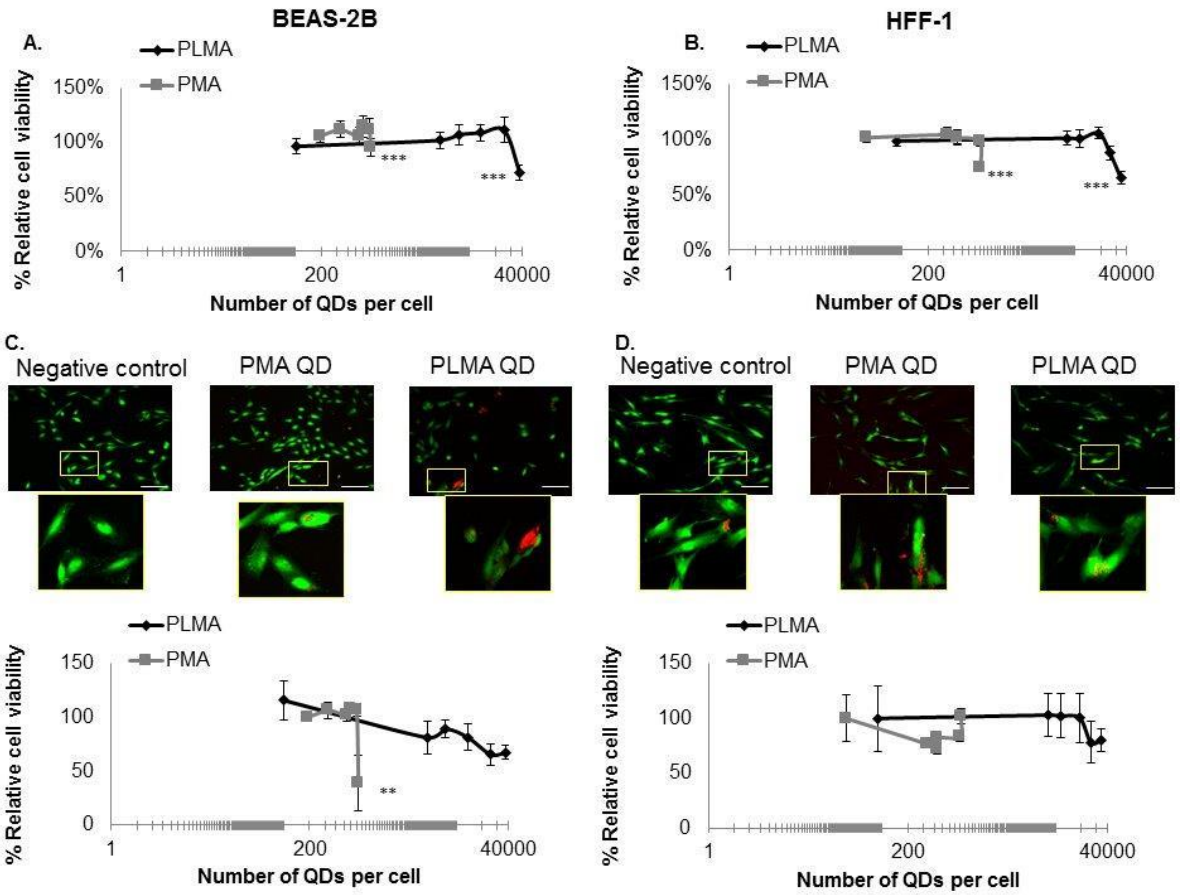

Figure 1. Cell viability results of A, C) BEAS-2B and B, D) HFF-1 cells exposed to various concentrations of PMA and PLMAQDs. A,B) Results shown for cells analyzed by the MTT assay. C,D) Results shown for high-content imaging analysis of cells exposed to QDs followed by staining for live cells (green) and dead cells (red). Quantitative data is shown for analysis of a minimum of 2000 cells per condition. Quantitative data are presented as mean $\pm$ SEM (n = 3) for QD-treated cells relative to untreated control cells (= 100%). The degree of statistical significance is shown when appropriate (*: $p < 0.05$, **: $p < 0.01$, ***: $p < 0.001$). The inset images are representative high-content images of control cells and cells stained with the respective QDs at 30 nM (scale bar = 10μm).

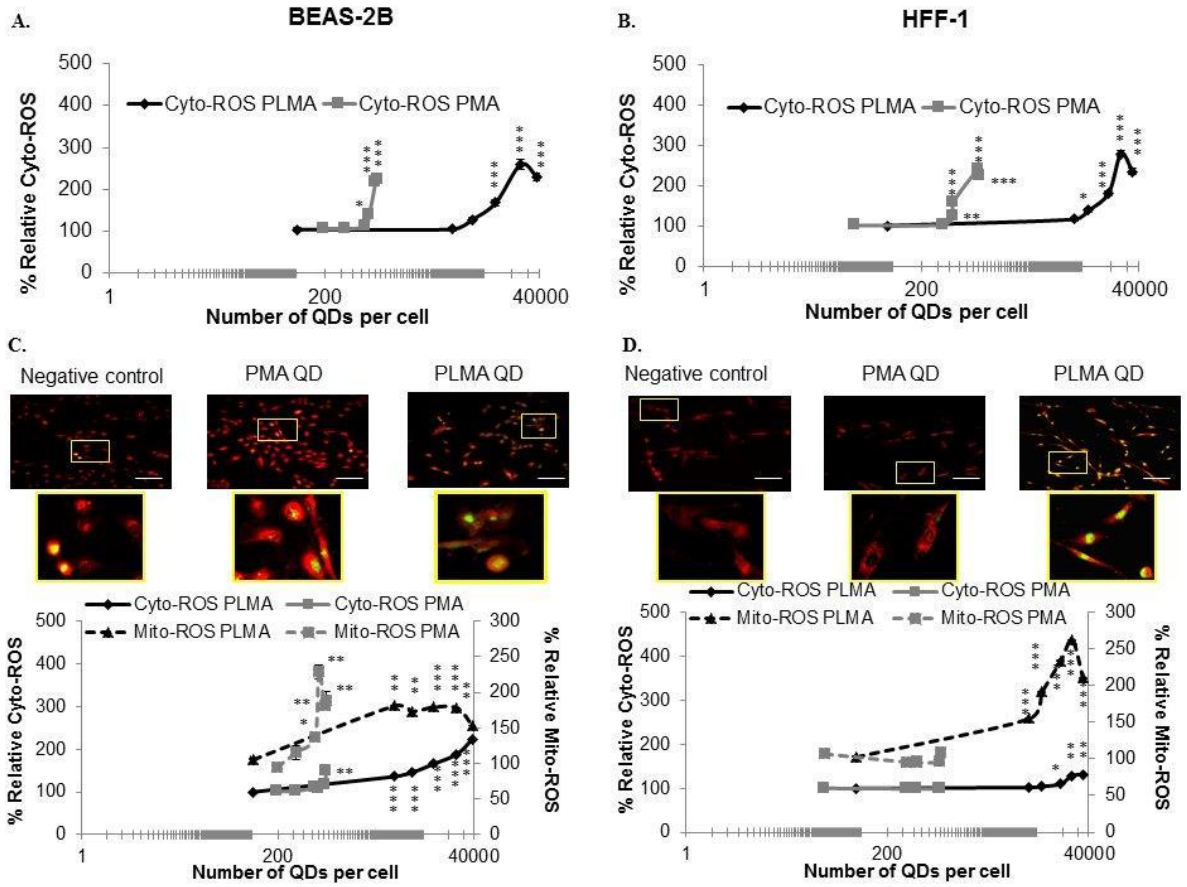

Figure 2. Induction of ROS by PLMA and PMA QDs in A, C) Beas-2B and B, D) HFF-1 cells exposed to various concentrations of PMA and PLMA charged QDs for 24 h. A,B) Data shown for cytoplasmic ROS using a common platereader assay. C, D) Data shown for high-content imaging based results for cells stained with CellROX Green (cytoplasmic ROS) and MitoTracker Red CMXRos (mitochondrial ROS). Quantitative data is shown for analysis of a minimum of 2000 cells per condition. Quantitative data are presented as mean $\pm$ SEM (n = 3) for QD-treated cells relative to untreated control cells (= 100%). The degree of statistical significance is shown when appropriate (*: $p < 0.05$, **: $p < 0.01$, ***: $p < 0.001$). The inset images are representative high-content images of control cells and cells stained with the respective QDs at 30 nM. The inset images are representative high-content images of control cells and cells stained with the respective QDs at 30 nM (scale bar = 10 µm).

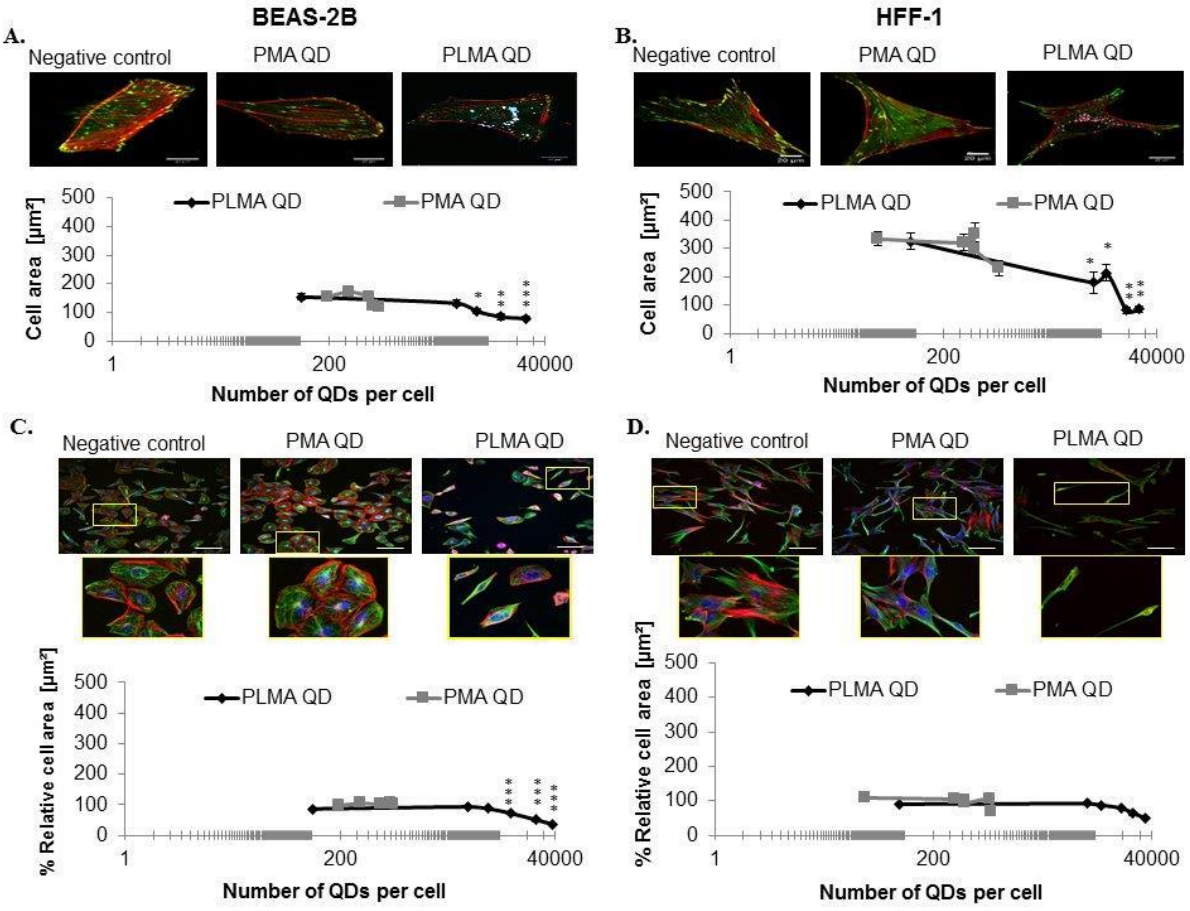

Figure 3. Cell morphology associated defects induced by QDs. (A, B) Representative images of confocal microscopy images of control cells and cells exposed to the respective QDs at 20 nM followed by staining for vinculin (green) and F-actin (red). Quantitative data is shown for analysis of a minimum of 15 cells per condition for Beas-2B cells and HFF-1 cells exposed to PLMA or PMAQDs for 24 h at various concentrations. (C, D) Control cells and cells exposed to the respective QDs up to 30 nM following high-content analysis of cells stained with CellMask (blue: cytoplasm), α-tubulin (green) and F-actin (red). Quantitative data are shown for analysis of a minimum of 2000 cells per condition for A) Beas-2B cells and B) HFF-1 cells exposed to PLMAor PMAQDs for 24 h at various concentrations. Quantitative data are presented as mean ± SEM (n = 3) for QD-treated cells relative to untreated control cells (= 100%). The degree of statistical significance is shown when appropriate (*: $p < 0.05$, **: $p <$

0.01, ***: $p < 0.001$). The inset images are representative high-content images of cells stained with the respective QDs at 20nM (confocal analysis, scale bar = 20μm) and 30 nM(InCell analysis, scale bar = 10μm).

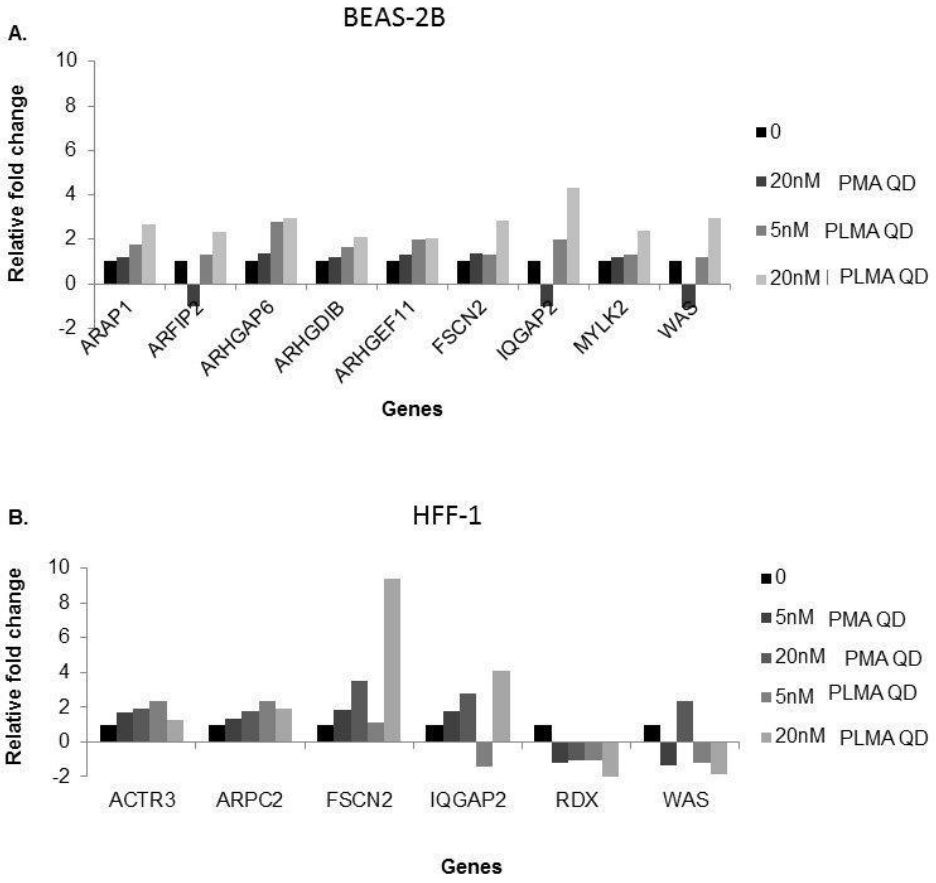

Figure 4. Relative gene expression levels in A) BEAS-2B and B) HFF-1 cells exposed to PLMA and PMA QDs at 0, 5 or 20 nM for 24 h. All genes tested are genes involved in cytoskeletal regulation and associated signaling. Only those genes are shown where significant up- or down-regulation was observed (change > 2-fold). Data are expressed as the fold-change in mean gene expression values normalized to the values obtained in untreated control cells (*n*= 1).

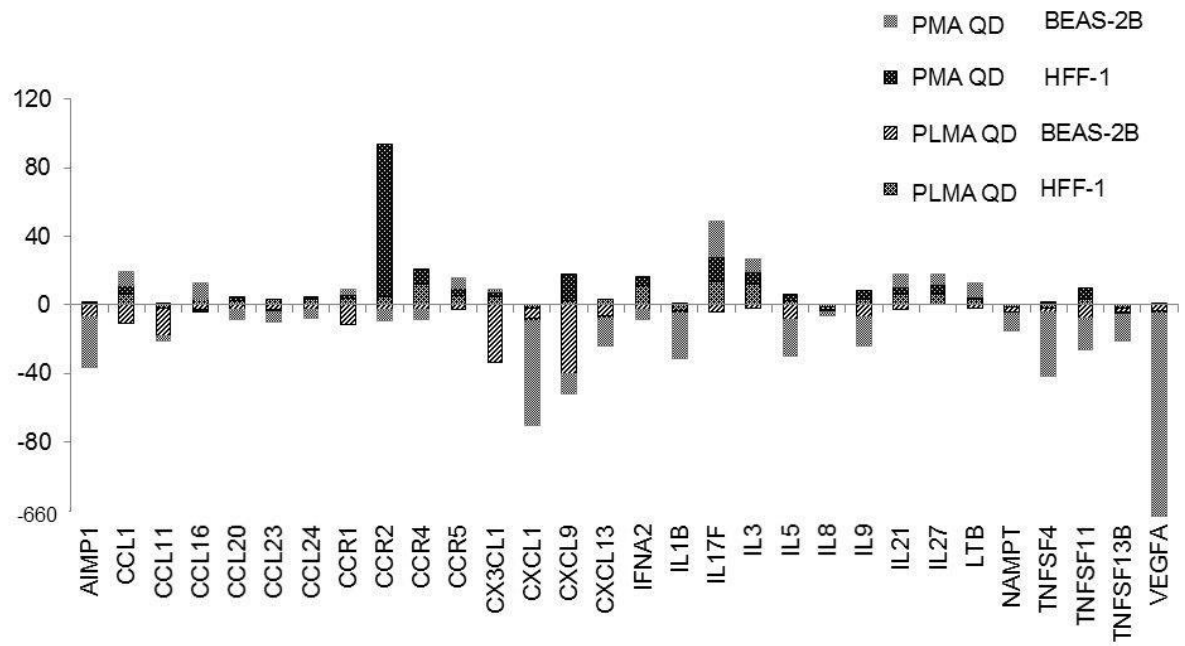

Figure 5. Relative gene expression levels for BEAS-2B and HFF-1 cells exposed to PLMA or PMA QDs at 20 nM. All genes tested are genes involved in inflammatory responses. Only those genes are shown where significant up- or down-regulation was observed (change > 5-fold). Data are expressed as the fold-change in mean gene expression values normalized to the values obtained in untreated control cells (n= 1).

Concentration in / Number of QDs per cell (*1000)	0	5	10	15	20	30
BEAS-2B cells PMA-QDs	**193**	**330**	**541**	**599**	**700**	**736**
% QDs internalized by cells		0.16%	0.13%	0.10%	0.09%	0.06%
BEAS-2B cells PLMA-QDs	**101**	**4602**	**7558**	**13539**	**24953**	**38534**
% QDs internalized by cells		2.29%	1.88%	2.25%	3.11%	3.20%
HFF-1 cells PMA-QDs	**38**	**333**	**433**	**435**	**796**	**813**
% QDs internalized by cells		0.17%	0.11%	0.07%	0.10%	0.07%
HFF -1 cells PLMA-QDs	**88**	**8299**	**11617**	**19038**	**25649**	**34192**
% QDs internalized by cells		4.13%	2.89%	3.16%	3.19%	2.84%

Table 1. ImageStream semi-quantitative image-based flow cytometry results for A) BEAS-2B and B) HFF-1 cells exposed to PLMAand PMA QDs at various concentrations (0 – 30 nM) for 24 h. The data indicate fluorescence intensity levels of control samples or QD-treated samples. The percentage of QDs internalized as determined by ICP-MS is also indicated.